



Article

Nox2 Upregulation and p38 α MAPK Activation in Right Ventricular Hypertrophy of Rats Exposed to Long-Term Chronic Intermittent Hypobaric Hypoxia

Eduardo Pena ^{1,2,*} , Patricia Siques ^{1,2} , Julio Brito ^{1,2} , Silvia M. Arribas ³, Rainer Böger ^{2,4} , Juliane Hannemann ^{2,4} , Fabiola León-Velarde ⁵, M. Carmen González ³, M. Rosario López ⁶ and Ángel Luis López de Pablo ³

¹ Institute of Health Studies, Universidad Arturo Prat, Avenida Arturo Prat 2120, Iquique 1110939, Chile; psiques@tie.cl (P.S.); jbritor@tie.cl (J.B.)

² Institute DECIPHER, German-Chilean Institute for Research on Pulmonary Hypoxia and Its Health Sequelae, Hamburg (Germany) and Iquique (Chile), Avenida Arturo Prat 2120, Iquique 1110939, Chile; boeger@uke.de (R.B.); j.hannemann@uke.de (J.H.)

³ Department of Physiology, University Autónoma of Madrid, Calle Arzobispo Morcillo 4, 28029 Madrid, Spain; silvia.arribas@uam.es (S.M.A.); m.c.gonzalez@uam.es (M.C.G.); angel.lopezdepablo@uam.es (Á.L.L.d.P.)

⁴ Institute of Clinical Pharmacology and Toxicology, University Medical Center Hamburg-Eppendorf, Martinistraße 52, 20246 Hamburg, Germany

⁵ Department of Biological and Physiological Science, Facultad de Ciencias y Filosofía/IIA, Cayetano Heredia University, Avenida Honorio Delgado 430, Lima 15102, Peru; fleon-velarde@concytec.gob.pe

⁶ Department of Preventive Medicine and Public Health, University Autónoma of Madrid, Calle Arzobispo Morcillo 4, 28029 Madrid, Spain; mrosario.lopez@uam.es

* Correspondence: eduardo.enrique.bio@gmail.com; Tel.: +5-657-252-6392

Received: 9 September 2020; Accepted: 9 October 2020; Published: 13 November 2020



Abstract: One of the consequences of high altitude (hypobaric hypoxia) exposure is the development of right ventricular hypertrophy (RVH). One particular type of exposure is long-term chronic intermittent hypobaric hypoxia (CIH); the molecular alterations in RVH in this particular condition are less known. Studies show an important role of nicotinamide adenine dinucleotide phosphate (NADPH) oxidase complex-induced oxidative stress and protein kinase activation in different models of cardiac hypertrophy. The aim was to determine the oxidative level, NADPH oxidase expression and MAPK activation in rats with RVH induced by CIH. Male Wistar rats were randomly subjected to CIH (2 days hypoxia/2 days normoxia; n = 10) and normoxia (NX; n = 10) for 30 days. Hypoxia was simulated with a hypobaric chamber. Measurements in the RV included the following: hypertrophy, Nox2, Nox4, p22phox, LOX-1 and HIF-1 α expression, lipid peroxidation and H₂O₂ concentration, and p38 α and Akt activation. All CIH rats developed RVH and showed an upregulation of LOX-1, Nox2 and p22phox and an increase in lipid peroxidation, HIF-1 α stabilization and p38 α activation. Rats with long-term CIH-induced RVH clearly showed Nox2, p22phox and LOX-1 upregulation and increased lipid peroxidation, HIF-1 α stabilization and p38 α activation. Therefore, these molecules may be considered new targets in CIH-induced RVH.

Keywords: oxidative stress; high altitude; cardiac hypertrophy; kinases and NADPH oxidase

1. Introduction

Exposure of individuals to high altitude usually results in decreased oxygen bioavailability in blood and tissues (hypobaric hypoxia) [1].

Altitude hypobaric hypoxia is classified according to the time of exposure, and there are three well-determined conditions: chronic hypobaric exposure, which represents people who live permanently at high altitude (Andes and Himalayas) [2] and acute exposure, which represents people who are exposed to high altitude for hours or few days (tourists and climbers). However, of particular interest is the growing number of individuals who are subjected to periods of work (days) at high altitude and rest (days) at sea level for years. This condition is completely different from other types of intermittent hypobaric hypoxia exposure (hours or seconds), such as in obstructive sleep apnea, training, and exercise, among other conditions [3]. Initially developed by studying mining activities in the north of Chile involving a great number of workers who were intermittently exposed to high altitude (3800 to 4600 m) for a long period of time, this condition is currently known throughout the world as “long-term chronic intermittent hypobaric hypoxia” exposure (CIH) [3,4].

Several studies have clearly established that hypobaric hypoxia exposure induces pulmonary hypertension [5–7] due to hypoxic pulmonary artery vasoconstriction [8,9], causing pulmonary artery remodeling and the subsequent development of pressure overload (PO)-induced right ventricular hypertrophy (RVH) [10–12]. In addition, this phenomenon has also been described in long-term CIH [13–15]. However, the molecular mechanisms underlying the development of RVH under this particular condition have yet to be determined.

Previous studies in animals [16] and humans [17] show that hypobaric hypoxia exposure induces oxidative stress in the heart. Moreover, oxidative stress has emerged as an important transducer of PO-induced cardiac hypertrophy [18–20]. In fact, several studies show that both hypobaric hypoxia and oxidative stress can activate kinase proteins, such as Akt and p38 α MAPK, and stabilize hypoxia-inducible transcription factor-1 α (HIF-1 α) [21,22], which are related to cardiac hypertrophy and ventricular remodeling [23–26].

One important contributor to oxidative stress in the heart is the nicotinamide adenine dinucleotide phosphate (NADPH) oxidase complex [20,27]. It is composed of seven catalytic isoforms termed Nox1 to Nox5 and Duox1/2 [28]. These isoforms of Nox are distinct according to their distribution in vivo, expression in cell types, locations in subcellular compartments, products, and functions in physiology and pathology [29]. For example, Nox2 and Nox4 isoforms are primarily expressed in the heart, with their p22phox subunit [18,27,30]. When these complexes (Nox) are activated, oxidative stress is produced through the exacerbated production of reactive oxygen species (ROS), which could result in damage to the cellular structure, such as lipid peroxidation [31]. However, it is important to highlight that Nox4 is constitutively active and is the only isoform of the Nox family involved in production of hydrogen peroxide (H₂O₂) as the main product [29]. The rest of Nox isoforms (Nox1, Nox2, Nox3, Nox5, Duox1 and Duox2) produce superoxide (O₂⁻) as the principal product [32], while Duox1/2 also produce H₂O₂ [33].

Despite this difference regarding oxidative products, it has been reported that Nox4 and Nox2 upregulation is related to cardiac hypertrophy [29]. This is supported by recent studies specifically involving RVH induced by other models of hypoxia (normobaric hypoxia) showing an upregulation of Nox2 and Nox4 through the activation of lectin-like oxidized low-density lipoprotein receptor-1 (LOX-1) [20]. These data highlight that LOX-1 can be activated not only by hypoxia but also by oxidized lipoprotein and shear stress [34,35]. Therefore, we hypothesized that Noxs (Nox2/4), p38 α MAPK and Akt kinase, HIF-1 α and LOX-1 would be overexpressed in CIH-induced RVH in rats, which we assessed in rats exposed to long-term CIH.

2. Results

2.1. Hematocrit and Ventricular Hypertrophy

At the end of the exposure period, the CIH rats exhibited higher Hct levels (64.3 \pm 1.9) than the NX group (44.1 \pm 2.3; p < 0.05) as expected.

The rats under CIH conditions showed significantly larger Fulton's index values than the rats under NX conditions ($p < 0.05$), which indicated the presence of RVH (Figure 1a). H&E staining revealed significantly enlarged right ventricular cardiomyocytes in the CIH group, supporting Fulton's index findings (Figure 1b,c).

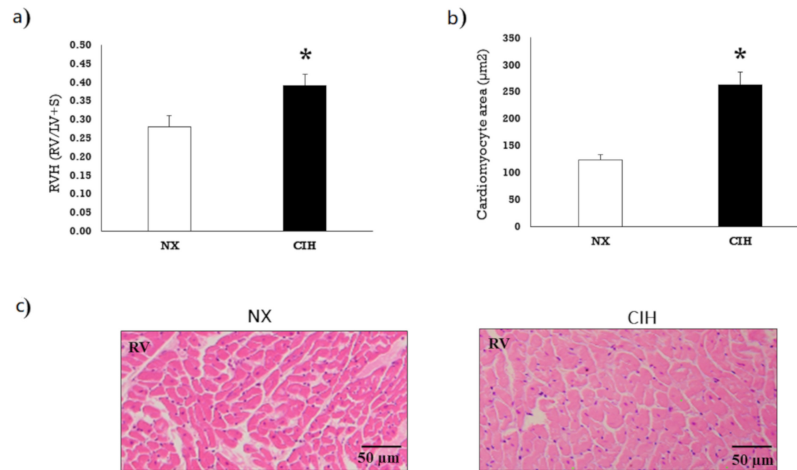


Figure 1. (a) Degree of right ventricle hypertrophy (RVH) by Fulton's index (right ventricle (RV)/left ventricle plus septum (LV+S)) after exposure to normoxia (NX; $n = 10$) and chronic intermittent hypobaric hypoxia (CIH; $n = 10$); (b) Cardiomyocyte area in the RV (μm^2); (c) Representative image of hematoxylin-eosin-stained RV tissue. The values are the mean (\bar{x}) \pm standard error (SE). * $p < 0.05$: CIH group vs. NX group.

2.2. LOX-1, Nox2, Nox4 and p22phox Expression

LOX-1 expression in the RV in the CIH group was moderately elevated compared to that in the NX group ($p < 0.05$) (Figure 2a). Nox2 expression in the RV was higher in the CIH group than in the NX group ($p < 0.05$) (Figure 2b). The protein expression of Nox4 in RV showed no differences among the groups (Figure 2c). Regarding the regulatory proteins, p22phox was significantly elevated in the CIH group ($p < 0.05$) compared to the NX group (Figure 2d).

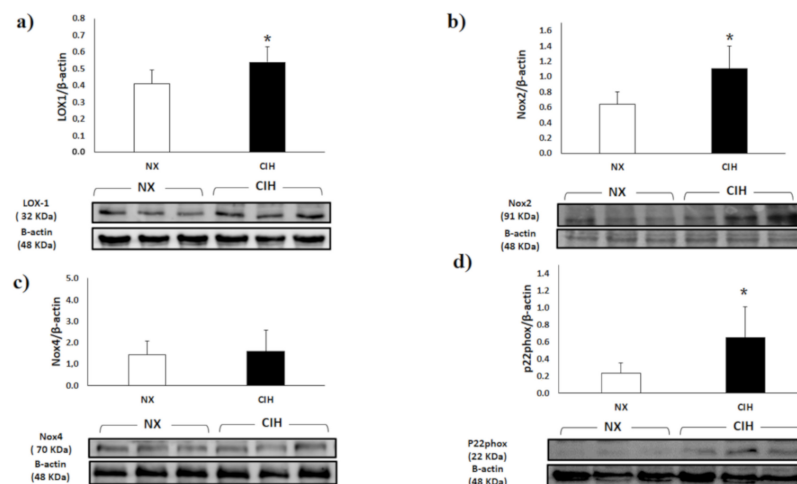


Figure 2. Expression of (a) Lectin-like oxidized low-density lipoprotein receptor-1 (LOX-1); (b) Nicotinamide adenine dinucleotide phosphate oxidase-2 (Nox2); (c) Nicotinamide adenine dinucleotide phosphate oxidase-4 (Nox4); (d) p22phox subunit (p22phox) expression in the right ventricle (RV) in the normoxia (NX; $n = 10$) and chronic intermittent hypobaric hypoxia (CIH; $n = 10$), groups, normalized by β -actin expression. Representative bands are shown. The values are the mean (\bar{x}) \pm standard error (SE). * $p < 0.05$: CIH group vs. NX group.

2.3. Lipid Peroxidation (MDA) Level and H₂O₂ Concentration

The concentration of lipid peroxides, expressed as the level of malondialdehyde (MDA), was higher in the RV tissue of the CIH group than in that of the NX group ($p < 0.05$) (Figure 3a). The hydrogen peroxide (H₂O₂) concentration in the RV tissue showed no differences between the groups; $p = \text{NS}$ (Figure 3b).

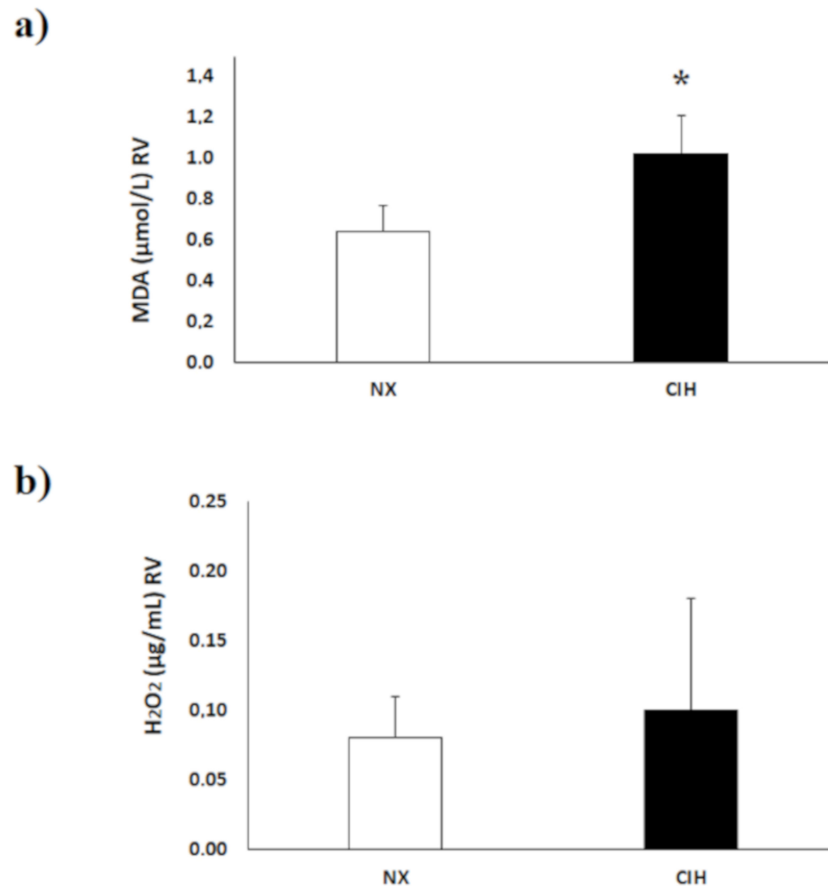


Figure 3. (a) Malondialdehyde (MDA) concentrations in the right ventricle tissue (RV); (b) hydrogen peroxide (H₂O₂) concentration in the RV under normoxia (NX); $n = 10$ and chronic intermittent hypobaric hypoxia (CIH); $n = 10$. The values are the mean (\bar{x}) \pm standard error (SE). * $p < 0.05$: CIH vs. NX group.

2.4. p38 α MAPK, Akt and HIF-1 α

p38 α MAPK activity in the RV of the CIH rat group was increased compared with that in the RV of the NX group (Figure 4a); The percentage of p38 activation in the CIH group was 54.1%, and that in the NX group was 43.4% ($p < 0.05$). Akt activation showed no differences among groups (Figure 4b); The percentage of Akt activation in CIH was 41.9%, and that in the NX group was 40.8%. On the other hand, HIF-1 α protein expression was moderately increased in the CIH group compared with the NX group ($p < 0.05$) (Figure 4c).

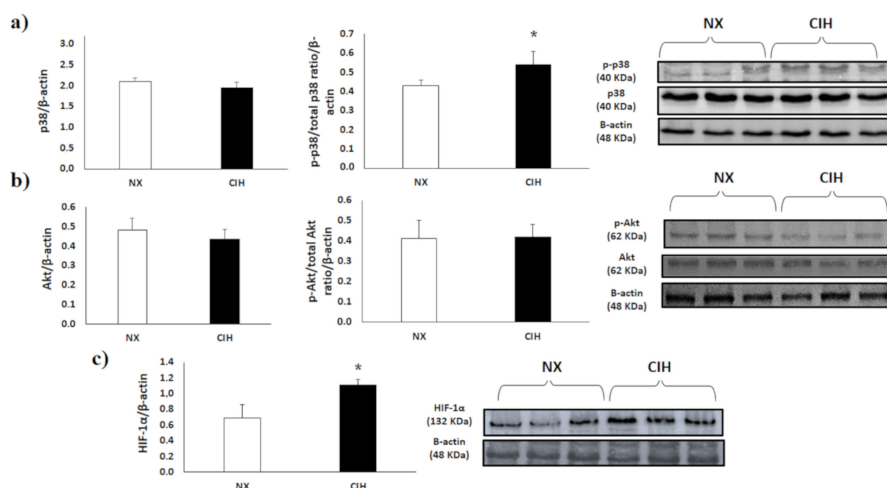


Figure 4. (a) Total p38 α expression and p38 α activity, assessed by the p-p38 α /p38 α ratio; (b) Total Akt expression and Akt activity assessed by the p-Akt/Akt ratio; (c) HIF-1 α expression in the right ventricle (RV), normoxia (NX; $n = 10$), chronic intermittent hypobaric hypoxia (CIH); $n = 10$. Protein levels were normalized to β -actin expression. Representative bands are shown. The values are the mean (\bar{x}) \pm standard error (SE). * $p < 0.05$: CIH vs. NX group.

3. Discussion

We explored some molecular pathways involved in RVH under CIH conditions. The results of this study show that exposure to CIH induces RVH concomitantly with increased lipid peroxidation, LOX-1, Nox2, p22phox and HIF-1 α expression, and p38 α MAPK activity.

Our first finding was the increase in Hct and development of RVH, which have been found mainly in chronic and lately in intermittent hypoxia [36–40]. In addition, an elevated Hct level has been described as an important factor in the development of RVH by an increase in viscosity [41]. In CIH, these findings of an increased Hct and RVH have also been described, but there is a paucity of data in the literature [40,42,43].

The role of oxidative stress in cardiac hypertrophy and some specific molecular mechanisms implicated have a growing body of evidence [11,20]. This current study showed an increased MDA concentration in CIH-induced RVH, which is consistent with the findings of other studies both in animals and humans in other types of hypoxia [16,17,44–46], highlighting increased lipid peroxidation. In addition, the levels of MDA or lipid peroxidation measures have been described as indirect but effective indexes of ROS generation [47]. Moreover, MDA interacts with kinases involved in cardiac hypertrophy, as will be discussed later.

As mentioned before, a study established an increase in Nox2 and Nox4 expression in cardiac hypertrophy under chronic normobaric hypoxia [20]. However, our results in CIH-induced RVH show an increase in Nox2 isoform expression and its essential component, p22phox, but there were no changes in Nox4 expression, which is not only different but also a novelty in the knowledge on RVH. The unchanged Nox4 expression level was concordant with the H₂O₂ level in RVH since Nox4 is the only isoform of the Nox family for the constitutive production of H₂O₂ [29,48]. However, the finding in this current study that hypertrophic right cardiac tissue did not show changes in Nox4 expression could be explained by studies that demonstrated that Nox4 is capable of inhibiting cardiac hypertrophy by stimulating autophagy [26,49]. Moreover, it has been described that Nox4 is more prevalent in smooth muscle cells of the vascular system than in cardiac tissue [18,50–52].

Regarding the increased levels of MDA (lipid peroxidation) and not H₂O₂, this could be due to the Harber-Weiss reaction, which is activated in different cell lines under oxidative stress conditions, producing an increase in hydroxyl radicals (OH) [53,54]. In addition, this OH is the principal molecule that triggers the initiation of lipid peroxidation production through nonsaturated lipids [55], generating an increase in MDA.

On the other hand, a study showed that the deletion of Nox2 decreased oxidative stress and HIF-1 α expression in cardiomyocyte cultures under normobaric hypoxia [56]. Although the latter study evaluated another type of hypoxia, it might support our findings regarding the upregulation of Nox2 and HIF-1 α in RVH under CIH conditions.

Regarding the possible participation of LOX-1 as a cardiac hypertrophy inducer in CIH-induced RVH, it has been suggested that LOX-1 expression can be upregulated by multiple factors, such as hypoxia, oxidized low-density lipoprotein and shear stress [57]. Moreover, a recent study showed that in chronic normobaric hypoxia-induced RVH the levels of NADPH oxidase were strongly increased through LOX-1 [20], which could support the increased expression of LOX-1 and Nox2 found in RVH under this particular type of hypoxia.

p38 α MAPK and Akt have been identified as redox-sensitive kinases and as main mediators of cardiac hypertrophy [58–60]. However, our data do not show Akt activation, which could suggest that this protein is not related to RVH under this particular exposure. On the other hand, the hypertrophied RV under study highlights an increase in p38 α MAPK activity. This result is consistent with studies showing an increase in p38 α activity through an increase in lipid peroxidation in other hypoxia models [61,62]. It is important to highlight that p38 presents four isoforms, α , β , γ (also known as Erk6 or SAPK3), and δ (also known as SAPK4), and their expression depends on the tissue and the cardiac process, where p38 α has been related to cardiac ventricular hypertrophy [63]. In addition, a study in mice under other types of hypoxia (chronic normobaric hypoxia, 10% O₂) showed that animals with PO-induced RVH exhibited increased p38 α expression, which was related to several effects, such as increased collagen and smooth muscle actin α (α -SMA) content leading to cardiac fibrosis [64].

In our current study, HIF-1 α protein was stabilized in the RVH induced by CIH. We hypothesized that HIF-1 α stabilization found in this experimental model could be related to p38 α activation since studies have shown that HIF-1 α stabilization in RVH under hypoxic conditions is due to p38 α activation [65,66]. In addition, the activation of p38 MAPK could be mediated by lipid peroxidation-produced MDA [61]. However, to corroborate this hypothesis, more studies are needed.

On the other hand, studies involving other hypoxic conditions (chronic hypobaric hypoxia) have shown that the activation of PKC ϵ (Ca²⁺-independent PKC isoform) represents an adaptive and protective role, abolishing mitochondrial impairment in the heart tissue [67]. However, a study in rats with RVH induced by the same hypoxic condition (chronic hypobaric hypoxia) showed an increase in the activation of PKC α [68], where PKC α produced an increase in gelatin-3 expression, which is related to cardiac fibrosis and heart failure [69]. Therefore, the assessment of the mechanistic activity and expression of PKC isoforms in RVH under this particular condition (CIH) is very interesting for future studies. In addition, regarding this type of condition, an interesting study by Brown et al. [70] showed that mice with RVH induced by chronic hypobaric hypoxia showed a relation of MAP kinase kinase-2 (MEKK-2) and the ERK5 pathway, leading to an increase in inflammatory molecules that triggered the cardiac hypertrophy process.

Moreover, it is important to highlight that a recent study in rats exposed to a chronic hypobaric hypoxia indicate that the RV differed from the left ventricle both in immune cells and expression of certain genes; therefore, this suggests that the two ventricles differ in aspects of pathophysiology and in potential therapeutic targets for RV dysfunction [71]. While these studies are not fully comparable to the hypoxic conditions in the current study, they provide new avenues to surmise hypothetical similar changes under CIH and future targets of study.

Regarding metabolic factors, two interesting studies by Muthuramu et al. [72,73] in another hypertrophy model, transverse aortic constriction (TAC), showed through cholesterol and homocysteine lowering gene therapy the pivotal role of cholesterol and homocysteine levels in the development of metabolic cardiac hypertrophy, fibrosis and heart function related to oxidative stress and protein kinase activation. Therefore, it is important to consider these pathways mentioned above in future studies since they could be present in the development of RVH induced under this particular condition of hypobaric hypoxia.

Our study attempted to present a preliminary overview of some key proteins that could be involved in long-term CIH-induced RVH compared to NX. We evidenced the presence of redox activity and some alterations in the main proteins known to be involved in cardiac hypertrophy. The information provided is rather novel because, to our knowledge, there is no information about the oxidative level and p38 activation in this particular kind of exposure to hypoxia in RVH.

Finally, a schematic diagram of the proposed signaling pathway that might be involved in the development of RVH induced by long-term intermittent hypobaric hypoxia exposure, is shown in Figure 5.

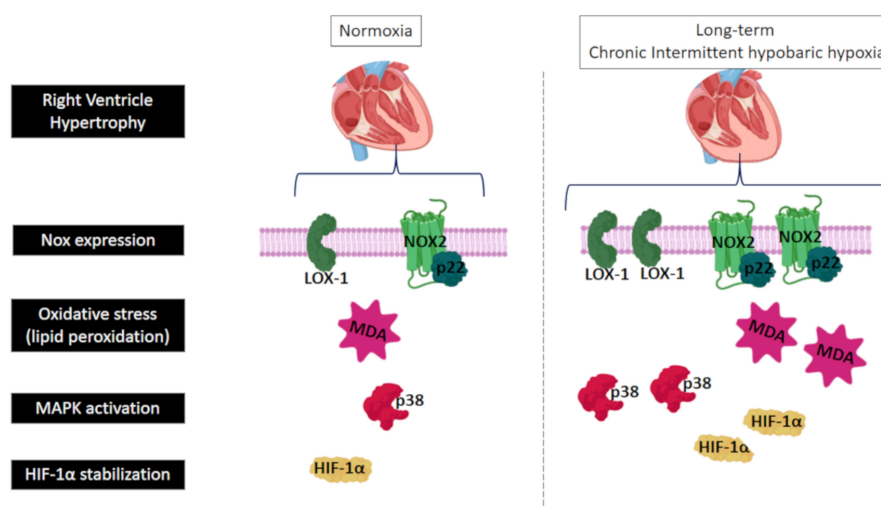


Figure 5. Schematic diagram of the main results and the proposed signaling pathway implicated in the development of right ventricle hypertrophy (RVH) induced by long-term intermittent hypobaric hypoxia; LOX-1: lectin-like oxidized low-density lipoprotein receptor-1; Nox2: nicotinamide adenine dinucleotide phosphate oxidase-2; p22: p22phox subunit of NADPH-oxidases; MDA: malondialdehyde; HIF-1 α : hypoxia-inducible factor-1 α , and p38 α : mitogen-activated protein kinase p38 α .

In conclusion, long-term CIH-induced RVH seems to be mediated by oxidative stress and redox signaling due to elevated lipid peroxidation, LOX-1, Nox2 and p22phox expression, p38 α MAPK activation, and HIF-1 α stabilization. These findings expand the general knowledge about protein alterations during CIH-induced RVH and open new avenues for the study of RVH in this particular hypoxic condition.

4. Materials and Methods

4.1. Study Groups

Twenty male Wistar rats (3 months old) were obtained from the animal facility of the Institute of Health Studies of Arturo Prat University, Iquique, Chile. The animal protocols and all other procedures were performed in accordance with the ethical standards for the handling of experimental animals (Chilean Law 20.380, Art 7, 3 Oct 2009) and were approved by the Research Ethics Committee of Arturo Prat University, Iquique, Chile (3 Jun 2015).

Rats were placed in individual cages at a temperature of 22 ± 2 °C with a circadian rhythm of 12 h of light and 12 h of darkness. Feeding consisted of 15 g/day of food that contained 22.0% crude protein, 5.0% crude fiber, 9.0% ash and 12% moisture (5POO[®], LabDiet, Prolab RMH3000), and water was given ad libitum. Movement inside the cage was not restricted, but no exercise was performed.

The rats were randomly distributed into 2 experimental groups: a normobaric normoxia (NX) group, which served as the sea level control group (n = 10), and a CIH group with 2 days of exposure to hypobaric hypoxia alternating with 2 days of exposure to NX (n = 10).

4.2. Animal Model

The exposure time for each group was 30 days, and hypobaric hypoxia was established in a hypobaric chamber at 428 Torr, which is equivalent to the pressure at an altitude of 4,600 m above sea level (the time to reach the final pressure was 60 min). In the chamber, the internal air flow rate was 3.14 L/min, and the humidity was between 21 and 30%. The NX group rats were kept in the same chamber room under the same environmental conditions except for hypobaric hypoxia. This protocol was previously validated, and it is a model that, despite the limitations of animal models, more closely mimics the conditions of exposure to long-term CIH in humans [40,74]. All experimental procedures were performed at the end of the 30-day exposure time. On day 30, the rats were anesthetized with ketamine (0.6 mg/kg BW) to obtain blood samples. Thereafter, the rats were euthanized through fatal thoracotomy, and the hearts were removed.

4.3. Biomedical Variables

Body weight (BW; g) and hematocrit percentage (Hct; %) were measured at the beginning and end of the exposure period. BW was measured with an electronic balance (Acculab V-1200[®], Lake Country, Illinois, USA). Blood samples were obtained by cardiac puncture in rats under anesthesia (0.3 mg of ketamine/kg BW) in heparinized vials. To determine the Hct, 1 mL of blood was transferred to a glass capillary tube and centrifuged at 5000 rpm for 5 min at 4 °C (Centrifuge 5804 R, Eppendorf AG[®], Hamburg, Germany).

4.4. Ventricular Hypertrophy

The hearts were removed; the right ventricle (RV) was detached and weighed, immediately frozen in liquid nitrogen and stored at −80 °C. RVH was determined by Fulton's index (the ratio of the right ventricular weight (g) to the left ventricular plus septum weight (g)), as described previously [75]. Moreover, histological analyses were performed. Ventricular tissue was fixed in 4% paraformaldehyde at room temperature overnight and then dehydrated and embedded in paraffin. Paraffin-embedded tissue slices (5 µm thick) were routinely stained with hematoxylin-eosin (H&E) for evaluation of the morphology and sizes of cardiac cells under light microscopy. The cell areas (µm²) were measured with ImageJ software (ImageJ 1.48 v, National Institutes of Health, USA).

4.5. Lipid Peroxidation

Lipid oxidation in ventricular tissues was assessed through determination of malondialdehyde (MDA) concentrations (µmol/L) using a colorimetric assay. First, 30 mg of RV was homogenized in 400 µL of RIPA buffer (50 mM Tris-HCl, Triton X-100 1%, 150 mM NaCl, and 0.1% SDS) for 2 min at 4000 rpm with a homogenizer (Stir-Pak[®], Brinton, IL, USA) at 4 °C. Then, 100 µL of the sample (plasma or homogenized tissue) was mixed with 200 µL of trichloroacetic acid (TCA; 10%) on ice for 30 min. Subsequently, the mixture was centrifuged at 4000 rpm for 15 min at 4 °C, and the supernatant (200 µL) was mixed with 200 µL of thiobarbituric acid (TBA; 0.67%) and incubated in a water bath (100 °C) for 1 h. Finally, the absorbance was measured with a spectrophotometer (Thermo Electron Corporation[®], Madison, Wisconsin, USA) at 532 nm. To ensure the reliability of the results, a calibration curve with MDA at known concentrations was created prior to the analysis.

4.6. Hydrogen Peroxide (H₂O₂) Determination

Quantification of H₂O₂ in the RV was performed on day 30 through a colorimetric method with a Hydrogen Peroxide (H₂O₂) Assay Kit (Elabscience Biotechnology Co., Ltd.[®], Wuhan, China) and a microplate reader (Infinite[®]200 PRO, TECAN[®], Mänedorf, Switzerland). The concentration of total protein was measured with a Bradford colorimetric method [76] with a BioPhotometer (Eppendorf AG[®], Hamburg, Germany) at 590 nm.

4.7. Western Blot Analysis

For protein extraction, 30 mg of tissue (RV) was first homogenized with 300 μ L of RIPA lysis buffer containing a cocktail of phosphatase and protease inhibitors (4 mM PMSF, 10 μ M leupeptin, 1 mM EDTA, 1 mM EGTA, 20 mM NaF, 20 mM HEPES, and 1 mM DTT). Then, the homogenates were centrifuged (Centrifuge 5804 R, Eppendorf AG[®], Hamburg, Germany) at 12,000 rpm for 20 min at 4 °C, and the supernatant was extracted. For quantification of total protein, the Bradford method was used [76] with a BioPhotometer (Eppendorf AG[®], Hamburg, Germany) at 590 nm. The protein extracts were stored at –80 °C. For Western blot analysis, the samples were diluted with 2 \times Laemmli buffer (0.125 M Tris-HCl, 4% (p/v) SDS, 20% (v/v) glycerol, 0.004% bromophenol blue, and 10% β -mercaptoethanol, pH 6.8). Proteins were separated according to their molecular weight (MW) under an electric field through sodium dodecyl sulfate polyacrylamide gel electrophoresis (SDS-PAGE) with 30% (v/v) bis-acrylamide. Then, the proteins were transferred from the SDS-PAGE gel to a polyvinylidene fluoride membrane (PVDF) with a semidry electroblotting system (OWL[™] Separation Systems, Panther Semi-Dry Electrobotters, Thomas Scientific[®], Barrington, Ill, USA).

Once the PVDF membrane was blocked with bovine serum albumin (BSA), it was incubated with primary antibodies against LOX-1 (1:2000, no. ab60178, Lot. No. GR3250577-3, Abcam), p-Akt (1:2000, no. sc-33437, Lot. No. E0316, Santa Cruz Biotechnology[®]), Akt (1:3000, no. sc-z8312, Lot. No. J2615, Santa Cruz Biotechnology[®]), Nox2 (1:2000, no. sc-5827, Lot. No. B1214, Santa Cruz Biotechnology[®]), Nox4 (1:4000, no. sc-55142, Lot. No. F1810, Santa Cruz Biotechnology[®]), p38 α MAPK (1:2000, no. sc-535, lot. No. C1113, Santa Cruz Biotechnology[®]), p-p38 α MAPK (1:2000, no. sc-7975-R, Lot. No. A1312, Santa Cruz Biotechnology[®]), p22phox (1:4000, no. sc-20781, Lot. No. F1512, Santa Cruz Biotechnology[®]), HIF-1 α (1:2000, no. sc-10790, Lot. No. C2614, Santa Cruz Biotechnology[®]), and β -actin (1:2000, no. sc-13065, Lot. No. K1418, Santa Cruz Biotechnology[®]) overnight at 4 °C. p38 α and Akt activation was determined as the ratio between the phosphorylated and nonphosphorylated forms and normalized to β -actin expression.

Finally, the membrane was incubated with the following secondary antibodies: anti-mouse (1:2000, no. sc-516102, Lot. No. A2219, Santa Cruz Biotechnology[®]), anti-goat (1:2000, no. sc-2004, Lot. No. J0614, Santa Cruz Biotechnology[®]) and anti-rabbit (1:2000, no. sc-2357, Lot. No. C2818, Santa Cruz Biotechnology[®]) antibodies at dilutions in 3% BSA for 1 h at room temperature and visualized in a dark room with a chemiluminescence kit (Chemiluminescence West Pico[®], Super Signal Substrate, Thermo Scientific[®], Rockford, Ill, USA). Densitometry of the bands was performed with the ImageJ program and normalized to β -actin expression.

4.8. Data Analysis

All data were included in a database and analyzed using the SPSS program (IBM SPSS[®] V.21.0, Armonk, NY, USA). The normality of the variables was established with the Kolmogorov-Smirnov test; all variables were found to be normally distributed. The mean and standard error (SE) were calculated for each variable. To establish intergroup differences, Student's t-test was used. The level of significance was $p < 0.05$.

Author Contributions: E.P., P.S. and J.B. conceived and designed the study, performed the experiments, analyzed and interpreted the data and provided overall supervision. Á.L.L.d.P., F.L.-V., R.B., J.H., S.M.A., M.R.L. and M.C.G. assisted in critical decisions and contributed to the interpretation of the results. All authors have read and agreed to the published version of the manuscript.

Funding: This study was supported by grants from GORE FIC-Tarapacá (BIP30487388-0), Arturo Prat University (IQUD17REM) and the German Federal Ministry of Education and Research under grant 01DN17046 (DECIPHER).

Acknowledgments: We would like to thank Daniel Aguayo, Samia El Alam and Gabriela Lamas of the Institute of Health Studies, Universidad Arturo Prat, and José García of the Hospital of Iquique for their technical assistance and support in the laboratory.

Conflicts of Interest: The authors declare no conflict of interest.

Abbreviations

RV	Right ventricle
CIH	Long-term chronic intermittent hypobaric hypoxia
RVH	Right ventricle hypertrophy
CIH	Long-term chronic intermittent hypobaric hypoxia
TAC	Transverse aortic constriction
NADPH oxidase	Nicotinamide adenine dinucleotide phosphate oxidase
LOX-1	Lectin-like oxidized low-density lipoprotein receptor-1
PKC	Protein kinase C
MEKK-2	MAP kinase kinase kinase-2
HIF-1 α	Hypoxia-inducible factor-1 α
H ₂ O ₂	Hydrogen peroxide
MAPKs	Mitogen activated protein kinases
ROS	Reactive oxygen species
O ₂ ⁻	Superoxide
OH	Hydroxyl radical
NX	Normobaric normoxia
BW	Body weight
Hct	Hematocrit
RV	Right ventricle
MDA	Malondialdehyde
TCA	Trichloroacetic acid
TBA	Thiobarbituric acid
BSA	Bovine serum albumin

References

- Bärtsch, P.; Gibbs, J.S. Effect of altitude on the heart and the lungs. *Circulation* **2007**, *116*, 2191–2202. [[CrossRef](#)] [[PubMed](#)]
- Moore, L.G. Human genetic adaptation to high altitude. *High Alt. Med. Biol.* **2001**, *2*, 257–279. [[CrossRef](#)] [[PubMed](#)]
- Richalet, J.P.; Donoso, M.V.; Jiménez, D.; Antezana, A.M.; Hudson, C.; Cortès, G.; Osorio, J.; León, A. Chilean miners commuting from sea level to 4500 m: A prospective study. *High Alt. Med. Biol.* **2002**, *3*, 159–166. [[CrossRef](#)] [[PubMed](#)]
- West, J.B. Commuting to high altitude: Value of oxygen enrichment of room air. *High Alt. Med. Biol.* **2002**, *3*, 223–235. [[CrossRef](#)] [[PubMed](#)]
- Xu, X.Q.; Jing, Z.C. High-altitude pulmonary hypertension. *Eur. Respir. Rev.* **2009**, *18*, 13–17. [[CrossRef](#)] [[PubMed](#)]
- Dunham-Snary, K.J.; Wu, D.; Sykes, E.A.; Thakrar, A.; Parlow, L.R.G.; Mewburn, J.D.; Parlow, J.L.; Archer, S.L. Hypoxic pulmonary vasoconstriction: From molecular mechanisms to medicine. *Chest* **2017**, *151*, 181–192. [[CrossRef](#)] [[PubMed](#)]
- Hou, X.; Chen, J.; Luo, Y.; Liu, F.; Xu, G.; Gao, Y. Silencing of STIM1 attenuates hypoxia-induced PASMCs proliferation via inhibition of the SOC/Ca²⁺/NFAT pathway. *Respir. Res.* **2013**, *14*, 2. [[CrossRef](#)] [[PubMed](#)]
- Von Euler, U.S.; Liljestrand, G. Observations on the pulmonary arterial blood pressure in the cat. *Acta Physiol. Scand.* **1946**, *12*, 301–320. [[CrossRef](#)]
- Moudgil, R.; Michelakis, E.D.; Archer, S.L. Hypoxic pulmonary vasoconstriction. *J. Appl. Physiol.* **2005**, *98*, 390–403. [[CrossRef](#)] [[PubMed](#)]
- Peñaloza, D.; Sime, F. Chronic cor pulmonale due to loss of altitude acclimatization (chronic mountain sickness). *Am. J. Med.* **1971**, *50*, 728–743. [[CrossRef](#)]
- Penaloza, D.; Arias-Stella, J. The heart and pulmonary circulation at high altitudes. *Circulation* **2007**, *115*, 1132–1146. [[CrossRef](#)]
- León-Velarde, F.; Villafuerte, F.C.; Richalet, J.P. Chronic mountain sickness and the heart. *Prog. Cardiovasc. Dis.* **2010**, *52*, 540–549. [[CrossRef](#)] [[PubMed](#)]

13. Sarybaev, A.S.; Palasiewicz, G.; Usupbaeva, D.A.; Plywaczewski, R.; Maripov, A.M.; Sydykov, A.S.; Mirrakhimov, M.M.; Le Roux, H.; Kadyrov, T.; Zielinski, J. Effects of intermittent exposure to high altitude on pulmonary hemodynamics: A prospective study. *High Alt. Med. Biol.* **2003**, *4*, 455–463. [[CrossRef](#)] [[PubMed](#)]
14. Brito, J.; Siques, P.; Arribas, S.M.; López de Pablo, A.L.; González, M.C.; Naveas, N.; Arriaza, K.; Flores, K.; León-Velarde, F.; Pulido, R.; et al. Adventitial alterations are the main features in pulmonary artery remodeling due to long-term chronic intermittent hypobaric hypoxia in rats. *BioMed Res. Int.* **2015**, *2015*, 169841. [[CrossRef](#)]
15. Brito, J.; Siques, P.; López, R.; Romero, R.; León-Velarde, F.; Flores, K.; Lüneburg, N.; Hannemann, J.; Böger, R.H. Long-term intermittent work at high altitude: Right heart functional and morphological status and associated cardiometabolic factors. *Front. Physiol.* **2018**, *9*, 248. [[CrossRef](#)] [[PubMed](#)]
16. Nakanishi, K.; Tajima, F.; Nakamura, A.; Yagura, S.; Ookawara, T.; Yamashita, H.; Suzuki, K.; Taniguchi, N.; Ohno, H. Effects of hypobaric hypoxia on antioxidant enzymes in rats. *J. Physiol.* **1995**, *489*, 869–876. [[CrossRef](#)] [[PubMed](#)]
17. Jefferson, J.A.; Simoni, J.; Escudero, E.; Hurtado, M.E.; Swenson, E.R.; Wesson, D.E.; Schreiner, G.F.; Schoene, R.B.; Johnson, R.J.; Hurtado, A. Increased oxidative stress following acute and chronic high altitude exposure. *High Alt. Med. Biol.* **2004**, *5*, 61–69. [[CrossRef](#)]
18. Li, J.M.; Gall, N.P.; Grieve, D.J.; Chen, M.; Shah, A.M. Activation of NADPH oxidase during progression of cardiac hypertrophy to failure. *Hypertension* **2002**, *40*, 477–484. [[CrossRef](#)]
19. Lu, Z.; Xu, X.; Hu, X.; Zhu, G.; Zhang, P.; Van Deel, E.D.; French, J.P.; Fassett, J.T.; Oury, T.D.; Bache, R.J.; et al. Extracellular superoxide dismutase deficiency exacerbates pressure overload-induced left ventricular hypertrophy and dysfunction. *Hypertension* **2008**, *51*, 19–25. [[CrossRef](#)]
20. Zhu, T.T.; Zhang, W.F.; Luo, P.; Qian, Z.X.; Li, F.; Zhang, Z.; Hu, C.P. LOX-1 promotes right ventricular hypertrophy in hypoxia-exposed rats. *Life Sci.* **2017**, *174*, 35–42. [[CrossRef](#)] [[PubMed](#)]
21. Guzy, R.D.; Hoyos, B.; Robin, E.; Chen, H.; Liu, L.; Mansfield, K.D.; Simon, M.C.; Hammerling, U.; Schumacker, P.T. Mitochondrial complex III is required for hypoxia-induced ROS production and cellular oxygen sensing. *Cell Metab.* **2005**, *1*, 401–408. [[CrossRef](#)]
22. Li, K.; He, C. Gastric mucosal lesions in Tibetans with high-altitude polycythemia show increased HIF-1A expression and ROS production. *BioMed Res. Int.* **2019**, *2019*, 6317015. [[CrossRef](#)] [[PubMed](#)]
23. Fujio, Y.; Nguyen, T.; Wencker, D.; Kitsis, R.N.; Walsh, K. Akt promotes survival of cardiomyocytes *in vitro* and protects against ischemia-reperfusion injury in mouse heart. *Circulation* **2000**, *101*, 660–667. [[CrossRef](#)]
24. Emerling, B.M.; Plataniias, L.C.; Black, E.; Nebreda, A.R.; Davis, R.J.; Chandel, N.S. Mitochondrial reactive oxygen species activation of p38 mitogen-activated protein kinase is required for hypoxia signaling. *Mol. Cell. Biol.* **2005**, *25*, 4853–4862. [[CrossRef](#)]
25. Son, Y.; Kim, S.; Chung, H.T.; Pae, H.O. Reactive oxygen species in the activation of MAP kinases. *Methods Enzymol.* **2013**, *528*, 27–48. [[CrossRef](#)]
26. Sag, C.M.; Santos, C.X.; Shah, A.M. Redox regulation of cardiac hypertrophy. *J. Mol. Cell. Cardiol.* **2014**, *73*, 103–111. [[CrossRef](#)] [[PubMed](#)]
27. Octavia, Y.; Brunner-La Rocca, H.P.; Moens, A.L. NADPH oxidase-dependent oxidative stress in the failing heart: From pathogenic roles to therapeutic approach. *Free Radic. Biol. Med.* **2012**, *52*, 291–297. [[CrossRef](#)] [[PubMed](#)]
28. Lasseègue, B.; Sorescu, D.; Szoöcs, K.; Yin, Q.; Akers, M.; Zhang, Y.; Grant, S.L.; Lambeth, J.D.; Griendling, K.K. Novel gp91 phox homologues in vascular smooth muscle cells. *Circ. Res.* **2001**, *88*, 888–894. [[CrossRef](#)] [[PubMed](#)]
29. Guo, S.; Chen, X. The human Nox4: Gene, structure, physiological function and pathological significance. *J. Drug Target* **2015**, *23*, 888–896. [[CrossRef](#)] [[PubMed](#)]
30. Hingtgen, S.D.; Tian, X.; Yang, J.; Dunlay, S.M.; Peek, A.S.; Wu, Y.; Sharma, R.V.; Engelhardt, J.F.; Davisson, R.L. Nox2-containing NADPH oxidase and Akt activation play a key role in angiotensin II-induced cardiomyocyte hypertrophy. *Physiol. Genom.* **2006**, *26*, 180–191. [[CrossRef](#)]
31. Su, L.J.; Zhang, J.H.; Gomez, H.; Murugan, R.; Hong, X.; Xu, D.; Jiang, F.; Peng, Z.Y. Reactive oxygen species-induced lipid peroxidation in apoptosis, autophagy, and ferroptosis. *Oxid. Med. Cell. Longev.* **2019**, *2019*, 5080843. [[CrossRef](#)]

32. Rodiño-Janeiro, B.K.; Paradelo-Dobarro, B.; Castiñeiras-Landeira, M.I.; Raposeiras-Roubín, S.; González-Juanatey, J.R.; Alvarez, E. Current status of NADPH oxidase research in cardiovascular pharmacology. *Vasc. Health Risk Manag.* **2013**, *9*, 401–428. [[CrossRef](#)]
33. Forteza, R.; Salathe, M.; Miot, F.; Forteza, R.; Conner, G.E. Regulated hydrogen peroxide production by Duox in human airway epithelial cells. *Am. J. Respir. Cell Mol. Biol.* **2005**, *32*, 462–469. [[CrossRef](#)]
34. Ogura, S.; Shimosawa, T.; Mu, S.; Sonobe, T.; Kawakami-Mori, F.; Wang, H.; Uetake, Y.; Yoshida, K.; Yatomi, Y.; Shirai, M.; et al. Oxidative stress augments pulmonary hypertension in chronically hypoxic mice overexpressing the oxidized LDL receptor. *Am. J. Physiol. Heart Circ. Physiol.* **2013**, *305*, H155–H162. [[CrossRef](#)]
35. Taye, A.; El-Sheikh, A.A. Lectin-like oxidized low-density lipoprotein receptor 1 pathways. *Eur. J. Clin. Investig.* **2013**, *43*, 740–745. [[CrossRef](#)]
36. Monge, C.; León-Velarde, F. *El Reto Fisiológico de Vivir en los Andes*; IFEA, UPCH: Lima, Peru, 2003.
37. Reeves, J.T.; Leon-Velarde, F. Chronic mountain sickness: Recent studies of the relationship between hemoglobin concentration and oxygen transport. *High Alt. Med. Biol.* **2004**, *5*, 147–155. [[CrossRef](#)]
38. Villafuerte, F.C.; Cárdenas, R.; Monge, C.-C. Optimal hemoglobin concentration and high altitude: A theoretical approach for Andean men at rest. *J. Appl. Physiol.* **2004**, *96*, 1581–1588. [[CrossRef](#)]
39. León-Velarde, F.; Maggiorini, M.; Reeves, J.T.; Aldashev, A.; Asmus, I.; Bernardi, L.; Ge, R.L.; Hackett, P.; Kobayashi, T.; Moore, L.G.; et al. Consensus statement on chronic and subacute high altitude diseases. *High Alt. Med. Biol.* **2005**, *6*, 147–157. [[CrossRef](#)]
40. Siqués, P.; Brito, J.; León-Velarde, F.; Barrios, L.; Cruz, J.J.D.L.; López, V.; Herruzo, R. Time course of cardiovascular and hematological responses in rats exposed to chronic intermittent hypobaric hypoxia (4600 m). *High Alt. Med. Biol.* **2006**, *7*, 72–80. [[CrossRef](#)]
41. Groeneveldt, J.A.; de Man, F.S.; Westerhof, B.E. The right treatment for the right ventricle. *Curr. Opin. Pulm. Med.* **2019**, *25*, 410–417. [[CrossRef](#)]
42. Brito, J.; Siqués, P.; León-Velarde, F.; De La Cruz, J.J.; López, V.; Herruzo, R. Chronic intermittent hypoxia at high altitude exposure for over 12 years: Assessment of hematological, cardiovascular, and renal effects. *High Alt. Med. Biol.* **2007**, *8*, 236–244. [[CrossRef](#)]
43. Lüneburg, N.; Siques, P.; Brito, J.; Arriaza, K.; Pena, E.; Klose, H.; Leon-Velarde, F.; Böger, R.H. Long-term chronic intermittent hypobaric hypoxia in rats causes an imbalance in the asymmetric dimethylarginine/nitric oxide pathway and ROS activity: A possible synergistic mechanism for altitude pulmonary hypertension? *Pulm. Med.* **2016**, *2016*, 65785789. [[CrossRef](#)]
44. Bailey, D.; Davies, B.; Young, I.S.; Hullin, D.A.; Seddon, P.S. A potential role of free radical-mediated skeletal muscle soreness in pathophysiology of acute mountain sickness. *Aviat. Space Environ. Med.* **2001**, *72*, 513–521. [[CrossRef](#)]
45. Joanny, P.; Steinberg, J.; Robach, P.; Richalet, J.P.; Gortan, C.; Gardette, B.; Jammes, Y. Operation everest III (Comex'97): The effect of simulated severe hypobaric hypoxia on lipid peroxidation and antioxidant defence systems in human blood at rest and after maximal exercise. *Resuscitation* **2001**, *49*, 307–314. [[CrossRef](#)]
46. Moller, P.; Loft, S.; Lundby, C.; Olsen, N.V. Acute hypoxia and hypoxic exercise induce DNA strand breaks and oxidative DNA damage in humans. *FASEB J.* **2001**, *15*, 1181–1186. [[CrossRef](#)]
47. Gutteridge, J.M.C.; West, M.; Eneff, K.; Floyd, R.A. Bleomycin-iron damage to DNA with formation of 8-hydroxydeoxyguanosine and base propenals. Indications that xanthine oxidase generates superoxide from DNA degradation products. *Free Radic. Res. Commun.* **1990**, *10*, 159–165. [[CrossRef](#)] [[PubMed](#)]
48. Takac, I.; Schröder, K.; Zhang, L.; Lardy, B.; Anilkumar, N.; Lambeth, J.D.; Shah, A.M.; Morel, F.; Brandes, R.P. The E-loop is involved in hydrogen peroxide formation by the NADPH oxidase Nox4. *J. Biol. Chem.* **2011**, *286*, 13304–13313. [[CrossRef](#)]
49. Sciarretta, S.; Zhai, P.; Shao, D.; Zablocki, D.; Nagarajan, N.; Terada, L.S.; Volpe, M.; Sadoshima, J. Activation of NADPH oxidase 4 in the endoplasmic reticulum promotes cardiomyocyte autophagy and survival during energy stress through the protein kinase RNA-activated-like endoplasmic reticulum kinase/eukaryotic initiation factor 2 α /activating transcription factor 4 pathway. *Circ. Res.* **2013**, *113*, 1253–1264. [[CrossRef](#)]
50. Bengtsson, S.H.; Gulluyan, L.M.; Dusting, G.J.; Drummond, G.R. Novel isoforms of NADPH oxidase in vascular physiology and pathophysiology. *Clin. Exp. Pharmacol. Physiol.* **2003**, *30*, 849–854. [[CrossRef](#)]

51. Barman, S.A.; Chen, F.; Su, Y.; Dimitropoulou, C.; Wang, Y.; Catravas, J.D.; Han, W.; Orfi, L.; Szantai-Kis, C.; Keri, G.; et al. NADPH oxidase 4 is expressed in pulmonary artery adventitia and contributes to hypertensive vascular remodeling. *Arterioscler. Thromb Vasc. Biol.* **2014**, *34*, 1704–1715. [[CrossRef](#)]
52. Jarman, E.R.; Khambata, V.S.; Cope, C.; Jones, P.; Roger, J.; Ye, L.Y.; Duggan, N.; Head, D.; Pearce, A.; Press, N.J.; et al. An inhibitor of NADPH oxidase-4 attenuates established pulmonary fibrosis in a rodent disease model. *Am. J. Respir. Cell Mol. Biol.* **2014**, *50*, 158–169. [[CrossRef](#)]
53. Haber, F.; Weiss, J. Über die Katalyse des Hydroperoxydes. *Naturwissenschaften* **1932**, *20*, 948–950. [[CrossRef](#)]
54. Kehrer, J.P. The Haber-Weiss reaction and mechanisms of toxicity. *Toxicology* **2000**, *149*, 43–50. [[CrossRef](#)]
55. Gutteridge, J.M. Lipid peroxidation initiated by superoxide-dependent hydroxyl radicals using complexed iron and hydrogen peroxide. *FEBS Lett.* **1984**, *172*, 245–249. [[CrossRef](#)]
56. Yu, B.; Meng, F.; Yang, Y.; Liu, D.; Shi, K. NOX2 antisense attenuates hypoxia-induced oxidative stress and apoptosis in cardiomyocyte. *Int. J. Med. Sci.* **2016**, *13*, 646–652. [[CrossRef](#)]
57. Lü, J.; Mehta, J.L. LOX-1: A critical player in the genesis and progression of myocardial ischemia. *Cardiovasc. Drugs Ther.* **2011**, *25*, 431–440. [[CrossRef](#)]
58. Takano, H.; Zou, Y.; Hasegawa, H.; Akazawa, H.; Nagai, T.; Komuro, I. Oxidative stress-induced signal transduction pathways in cardiac myocytes: Involvement of ROS in heart diseases. *Antioxid. Redox Signal.* **2004**, *5*, 789–794. [[CrossRef](#)] [[PubMed](#)]
59. Takimoto, E.; Kass, D.A. Role of oxidative stress in cardiac hypertrophy and remodeling. *Hypertension* **2007**, *49*, 241–248. [[CrossRef](#)]
60. Oka, T.; Akazawa, H.; Naito, A.T.; Komuro, I. Angiogenesis and cardiac hypertrophy. *Circ. Res.* **2014**, *114*, 565–571. [[CrossRef](#)]
61. Folden, D.V.; Gupta, A.; Sharma, A.C.; Li, S.Y.; Saari, J.T.; Ren, J. Malondialdehyde inhibits cardiac contractile function in ventricular myocytes via a p38 mitogen-activated protein kinase-dependent mechanism. *Br. J. Pharmacol.* **2003**, *139*, 1310–1316. [[CrossRef](#)]
62. Yu, M.; Zheng, Y.; Sun, H.X.; Yu, D.J. Inhibitory effects of enalaprilat on rat cardiac fibroblast proliferation via ROS/P38MAPK/TGF- β 1 signaling pathway. *Molecules* **2012**, *17*, 2738–2751. [[CrossRef](#)]
63. Kumar, S.; Blake, S.M. Pharmacological potential of p38 MAPK inhibitors. In *Inhibitors of Protein Kinases and Protein Phosphates. Handbook of Experimental Pharmacology*; Pinna, L.A., Cohen, P.T., Eds.; Springer: Berlin/Heidelberg, Germany, 2005; pp. 65–83.
64. Kojonazarov, B.; Novoyatleva, T.; Boehm, M.; Happe, C.; Sibinska, Z.; Tian, X.; Sajjad, A.; Luitel, H.; Kriechling, P.; Posern, G.; et al. p38 MAPK inhibition improves heart function in pressure-loaded right ventricular hypertrophy. *Am. J. Respir. Cell Mol. Biol.* **2017**, *57*, 603–614. [[CrossRef](#)]
65. Gao, N.; Jiang, B.H.; Leonard, S.S.; Corum, L.; Zhang, Z.; Roberts, J.R.; Antonini, J.; Zheng, J.Z.; Flynn, D.C.; Castranova, V.; et al. p38 signaling-mediated hypoxia-inducible factor 1 α and vascular endothelial growth factor induction by Cr(VI) in DU145 human prostate carcinoma cells. *J. Biol. Chem.* **2002**, *277*, 45041–45048. [[CrossRef](#)]
66. Koodie, L.; Ramakrishnan, S.; Roy, S. Morphine suppresses tumor angiogenesis through a HIF-1 α /p38MAPK pathway. *Am. J. Pathol.* **2010**, *177*, 984–997. [[CrossRef](#)]
67. McCarthy, J.; Lochner, A.; Opie, L.H.; Sack, M.N.; Essop, M.F. PKC ϵ promotes cardiac mitochondrial and metabolic adaptation to chronic hypobaric hypoxia by GSK3 β inhibition. *J. Cell. Physiol.* **2011**, *226*, 2457–2468. [[CrossRef](#)]
68. Uenoyama, M.; Ogata, S.; Nakanishi, K.; Kanazawa, F.; Hiroi, S.; Tominaga, S.; Seo, A.; Matsui, T.; Kawai, T.; Suzuki, S. Protein kinase C mRNA and protein expressions in hypobaric hypoxia-induced cardiac hypertrophy in rats. *Acta Physiol.* **2010**, *198*, 431–440. [[CrossRef](#)]
69. Song, X.; Qian, X.; Shen, M.; Jiang, R.; Wagner, M.B.; Ding, G.; Chen, G.; Shen, B. Protein kinase C promotes cardiac fibrosis and heart failure by modulating galectin-3 expression. *Biochim. Biophys. Acta* **2015**, *1853*, 513–521. [[CrossRef](#)]
70. Brown, R.D.; Ambler, S.K.; Li, M.; Sullivan, T.M.; Henry, L.N.; Crossno, J.T., Jr.; Long, C.S.; Garrington, T.P.; Stenmark, K.R. MAP kinase kinase kinase-2 (MEKK2) regulates hypertrophic remodeling of the right ventricle in hypoxia-induced pulmonary hypertension. *Am. J. Physiol. Heart Circ. Physiol.* **2013**, *304*, H269–H281. [[CrossRef](#)]
71. Gorr, M.W.; Sriram, K.; Chinn, A.M.; Muthusamy, A.; Insel, P.A. Transcriptomic profiles reveal differences between the right and left ventricle in normoxia and hypoxia. *Physiol. Rep.* **2020**, *8*, e14344. [[CrossRef](#)]

72. Muthuramu, I.; Singh, N.; Amin, R.; Nefyodova, E.; Debasse, M.; Van Horenbeeck, I.; Jacobs, F.; De Geest, B. Selective homocysteine-lowering gene transfer attenuates pressure overload-induced cardiomyopathy via reduced oxidative stress. *J. Mol. Med.* **2015**, *93*, 609–618. [[CrossRef](#)]
73. Muthuramu, I.; Amin, R.; Postnov, A.; Mishra, M.; Aboumsallem, J.P.; Dresselaers, T.; Himmelreich, U.; Van Veldhoven, P.P.; Gheysens, O.; Jacobs, F.; et al. Cholesterol-lowering gene therapy counteracts the development of non-ischemic cardiomyopathy in mice. *Mol. Ther.* **2017**, *25*, 2513–2525. [[CrossRef](#)]
74. Brito, J.; Siqués, P.; León-Velarde, F.; Cruz, J.J.D.L.; Barlaro, T.; López, V.; Herruzo, R. Varying exposure regimes to long term chronic intermittent hypoxia exert different outcomes and morphological effects on Wistar rats at 4600 m. *Toxicol. Environ. Chem.* **2008**, *90*, 169–179. [[CrossRef](#)]
75. Kay, J.M. Effect of intermittent normoxia on chronic hypoxic pulmonary hypertension, right ventricular hypertrophy, and polycythemia in rats. *Am. Rev. Respir. Dis.* **1980**, *121*, 993–1001. [[CrossRef](#)]
76. Bradford, M.M. A rapid and sensitive method for the quantitation of microgram quantities of protein utilizing the principle of protein-dye binding. *Anal. Biochem.* **1976**, *72*, 248–254. [[CrossRef](#)]

Publisher’s Note: MDPI stays neutral with regard to jurisdictional claims in published maps and institutional affiliations.



© 2020 by the authors. Licensee MDPI, Basel, Switzerland. This article is an open access article distributed under the terms and conditions of the Creative Commons Attribution (CC BY) license (<http://creativecommons.org/licenses/by/4.0/>).